2483

FILTECH 2011
CONFERENCE PROCEEDINGS
VOLUME I

CONTENT VOLUME I

CONTENT VOLUME II

Conference Dates:
March 22 – 24, 2011

Venue:
Rhein-Main-Hallen · Rheinstr. 20 · 65028 Wiesbaden · Germany

Organizer:

Filtech Exhibitions Germany
PO Box 1225 · 40637 Meerbusch – Germany
phone: +49 (0) 2132 93 57 60
fax: +49 (0) 2132 93 57 62
e-mail: Info@Filtech.de
web: www.Filtech.de

ISBN 978-3-941655-011-0

TREATMENT OF HIGHLY VISCOUS LUBRICANTS BY HIGH GRADIENT MAGNETIC SEPARATION TECHNIQUE

Dipl.-Ing. Katharina Menzel*, Dipl.-Ing. Johannes Lindner,
Prof. Dr.-Ing. Hermann Nirschl
Institute of Mechanical Process Engineering and Mechanics (MVM),
Karlsruhe Institute of Technology (KIT), 76131 Karlsruhe, Germany,
Email: katharina.menzel@kit.edu

ABSTRACT

Abrasive particles in gear and hydraulic oils are decisively responsible for increased wear in machine elements like bearings or breakdown of entire machine systems, e.g. the gear in wind power plants. The monitoring of the lubricant condition as well as its continuous treatment is therefore essential to increase the lifetime of the equipment [1]. The separation of micrometer particles ranging from 1 to 20 µm of a high viscosity lubricant is still challenging in state of the art deep bed filtration because of high pressure drop and the unintentional separation of additives. It has been investigated that wear particles of different chemical composition are magnetisable and therefore Magnetic Separation is a promising approach to separate these particle clusters, while avoiding the separation of oil additives. The magnetic force is effective at great distance to the separating wire. The HGMS filter is therefore configurated much more porous than conventional filter material. Hence the pressure drop in High Gradient Magnetic Separation (HGMS) is negligible which is a great advantage and helps to decrease operating expenses.

KEYWORDS

High Gradient Magnetic Separation, Oil Filtration, Lubricant treatment, Viscosity, Scale-up

1. Introduction

At the Institute of Mechanical Process Engineering and Mechanics a regenerative magnetic separator based upon the HGMS principle (**H**igh **G**radient **M**agnetic **S**eparation) [2] has been developed. The method utilizes the magnetic force which is excited through the distortion of the external magnetic field by means of ferromagnetic wires. Next to the wire, high magnetic forces occur, causing magnetisable particles to adhere on it. The filtration effect of a HGMS apparatus has similarities with deep bed filtration, although the principle has further important benefits. The application of thin wires ensures the separation of small magnetisable particles of micro- and submicrometer scale. The magnetic force is effective even at a great distance from the wire (between 1- to 100-times the wire radius). Simultaneously, the porosity of the magnetic filter is therefore significantly higher than of a common deep bed filter. This allows any additives in the lubricating oil to pass unhindered, whereas they may be unintentionally separated in deep bed filters.

The paper presents the performance of the magnetic separator regarding the deposition of particles on two different diameter sized wires and on the separation efficiency as a function of the flow and the magnetic field strength of various single wire stages. The results will show the loading distribution of the matrix stages in dependency of their position within the HGMS filter apparatus. Another observation shows the separation grade of two different matrix arrangements.

2. Method

The separation apparatus, which is shown in demounted state in Figure 1 on the left side, is designed flexible in order to embed a conventional filter element or magnetisable HGMS filter elements (see Figure 2) into it. The designated number of HGMS filter elements is assembled inside of the apparatus. The distance between each filter element may be varied. In Figure 1 on the right side the system diagram is shown: The initial suspension is located inside a heated and stirred feed reservoir. The peristaltic pump feeds the suspension into the HGMS filter which is located in the centre of an electromagnetic coil. In single-pass test the fluid flows into the collecting tray, where the weight is measured using a balance. In multi-pass test, the suspension is pumped in closed loop as in this way filters are applied in industrial oil circuits.

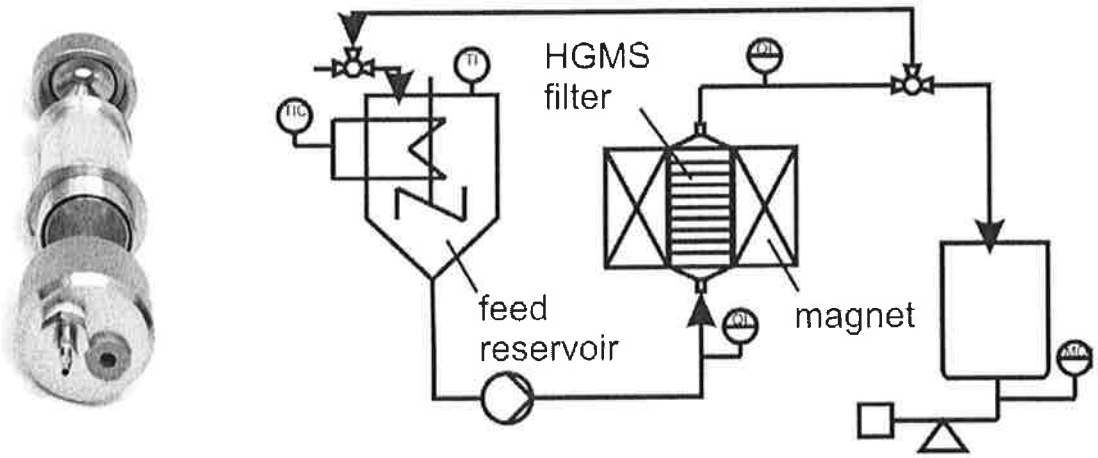

Figure 1: left: separation device in demounted state, right: test flow diagram

For the trials wire mesh stages of the magnetic ferrite stainless chromium steel DIN 1.4016 have been produced. Their internal diameter is 30 mm and they are characterized by the wire diameter *d* and the mesh width *w*. The denotation in this paper is made by (wire diameter *d*/ mesh width *w*) in millimetres, eg. (0,2/1).

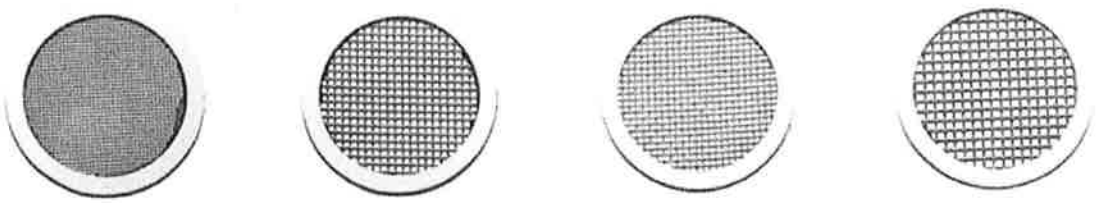

d/*w* = 0,25/0,375 *d*/*w* = 0,4/1 *d*/*w* = 0,2/1 *d*/*w* = 0,4/1,4

Figure 2: HGMS wire mesh stages with the diameter of the wire *d* and the mesh width *w* in mm

In context of the wire mesh geometry the dimensionless specific surface area Φ is introduced as additional parameter for comparison between the mesh stages. It is defined as [3]:

$$\phi = d\frac{A_S}{V} = d\frac{\pi \cdot l_D}{(w+d)^2} \approx \frac{\pi \cdot d \cdot \sqrt{d^2 + (w+d)^2}}{(w+d)^2} \qquad (1)$$

where A_s is the surface area of the wire mesh, V is the volume of the mesh and l_D *is* the wire length. The dimensionless specific surface area Φ can be expressed by the diameter of the wire *d* and the mesh width *w* if the enlacement of the wire is neglected. The dimensions of the matrices and their dimensionless specific surface area Φ are shown in Table 1.

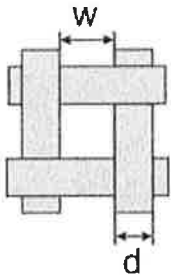

Figure 3: Wire mesh geometry

Table 1: Dimensions of the HGMS filter matrix elements

Wire mesh	Wire diameter *d* [mm]	Mesh width *w* [mm]	Dimensionless specific surface area Φ [-]
0,25/0,375	0,25	0,375	1,35
0,4/1	0,40	1,000	0,93
0,4/1,4	0,40	1,400	0,72
0,2/1	0,22	1,000	0,53

The deposition on the filter matrix element is determined gravimetrically. After completing the test, the oil in the filter cartridge is emptied and the filter matrix elements are placed separately into bowls. Subsequently, the detachment of the particle with solvent in an ultrasonic bath is realized and the particle- solvent suspension is filtered through a membrane filter of 0,2 µm. The weight of the membrane is determined before and after filtration using a high precision balance. The separation efficiency is defined as

$$E = (1 - \frac{c_{filtrate}}{c_{feed}}) * 100\% \qquad (2)$$

where *c* is the concentration of the feed and filtrate, respectively.

The separation grade *G* indicates the separation efficiency as a function of the particle size *x*. It is possible to read from the separation grade which particles of a certain size fraction are separated and which remain in the filtrate. The separation grade G is defined as follows:

$$G(x_m) = (1 - \frac{q_{3,filtrate}(x_m)}{q_{3,feed}(x_m)} f) * 100\% \qquad \text{with } f = \frac{c_{filtrate}}{c_{feed}} \qquad (3)$$

with the volume density distribution q_3 as a function of the equivalent median particle diameter x_m of the feed and filtrate, respectively. *f* is the filtrate proportion, hence the ratio of the particle concentration in the filtrate to that in the feed.

3. Materials

As the filtration of micro- and submicrometer particles is a sophisticated task in deep bed filtration, the following test material was selected. Bayoxid E8709 particles from LANXESS consist of pure synthetically produced magnetite (Fe_3O_4). Its properties are listed in Table 2.

Table 2: Characteristics of the particles

Name	Saturation magnetization [Am²/kg]	Density [kg/m³]	BET Specific surface area [m²/g]
Bayoxid E8709	94	5090	5,94

The SEM image which is shown in Figure 4 demonstrates that the particle shape is partly round and rectangular and that they form large aggregates. The measurement of particle size is by laser light diffraction. The volume density distribution q_3 of magnetic particles is shown in Figure 5. The average diameter is 3,5 µm.

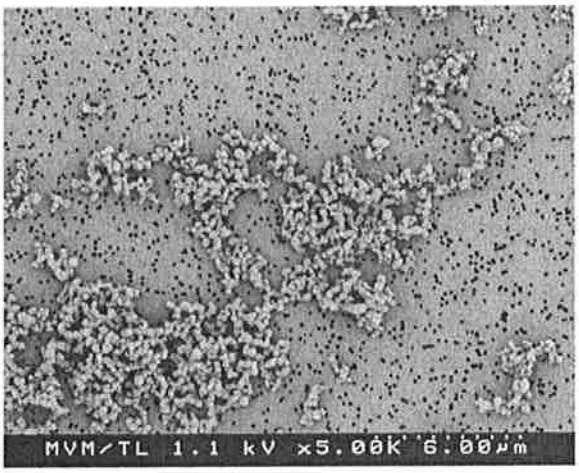

Figure 4: Scanning electron microscopy image of Bayoxid E8709 particles

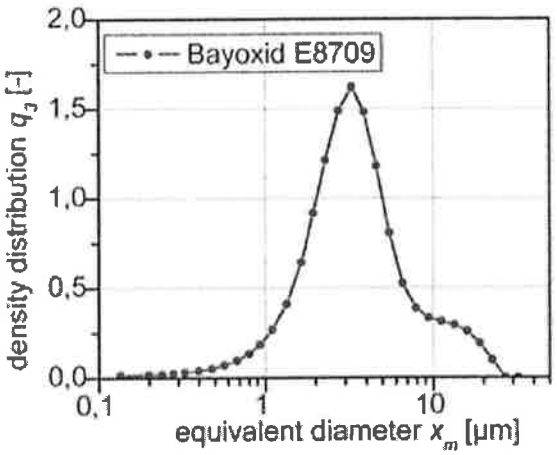

Figure 5: Particle size distribution of Bayoxid E8709 particles

As test media FVA2 oil, a mineral oil (Weber Reference Oils, www.reference-oils.com) was used. The oil has no additives and is available as reference oil. It is applied because its viscosity at test temperature of 20° C, correspond to that of the gear oil at operation temperature of 60°C. The density of the oil is 866 kg/cm³ at 20°C. In Figure 6 viscosity measurements as a function of temperature (from 10°C to 30°C) are shown. The viscosity decreases when temperature rises. Owing to Arrhenius approach the dynamic viscosity η can be calculated as a function of the temperature *t:*

$$\eta = \eta_0 + A1 \cdot exp(-t / b) \qquad (4)$$

The constants η, *A1* and *b* determined for the oil are provided in Figure 6.

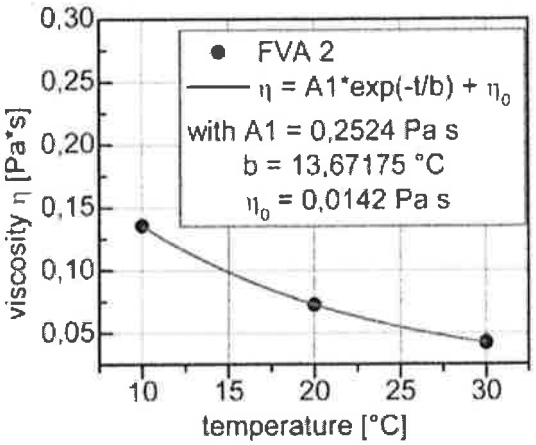

Figure 6: Viscosity measurement of the oil FVA 2 and the constants of Arrhenius approach

4. Results

Deposition of magnetic particles on a single wire

The deposition of magnetic particles on a single wire using an endoscopic video camera is shown in Figure 7.

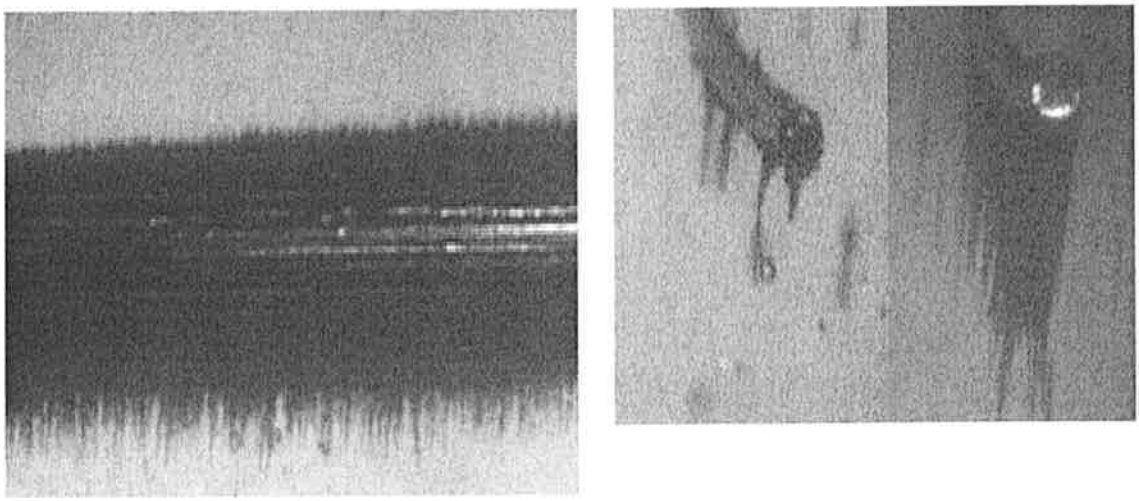

Figure 7: Observation of the particle deposition on a single wire using an endoscopic video camera

The left image in Figure 7 shows a longitudinally taut wire, on which particles are deposited at the bottom and on the top of it. The pictures on the right side in Figure 7 show a wire cross section at the beginning of the deposition (left) and at the time of saturation loading (right). At the time of saturation, the addition level is determined by a wire of radius 0,1 mm and 0,25 mm. The results in dependency of the volume flow of these measurements are shown in Figure 8.

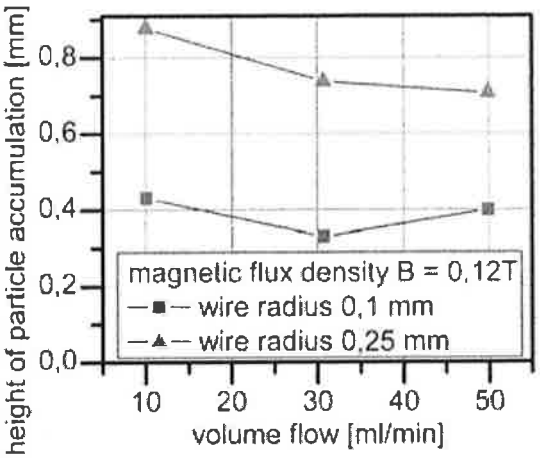

Figure 8: Particle accumulation height of a wire of radius 0,1 mm and 0,25 mm at saturation

Due to the data in Figure 8 it is evident that the particle loading amount on the thin wire (rectangular symbols) is less than on the thicker wire (triangular symbols). This means that the specific mass loading capacity of the wire increases for larger radius.

Single filter matrix stage

The performance of the magnetic separator regarding the separation efficiency as a function of the flow and the magnetic field strength is evaluated by using a single wire stage.

The experiments were conducted in single- pass and the filtrated volume was kept equal. A single wire mesh stage is arranged in the centre of the filter apparatus.

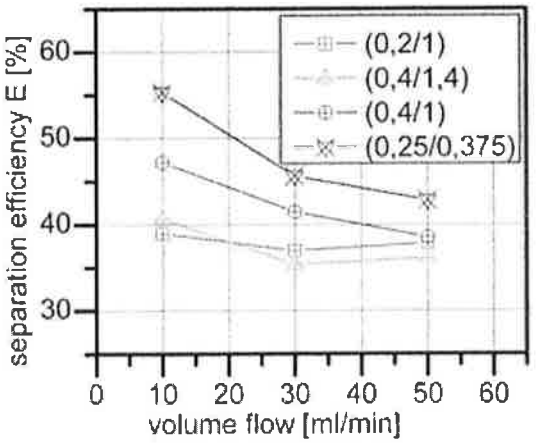

Figure 9: Removal efficiency of single wire mesh at increasing flow rate and constant magnetic flux density (B = 0,12 T)

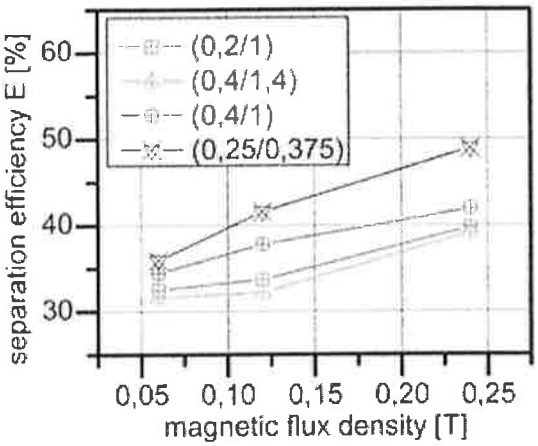

Figure 10: Removal efficiency of single wire mesh at increasing magnetic flux density and constant flow rate (30 ml/min)

The volume flow and the magnetic field density were varied in the experiments. The particle concentration of the feed is kept constant at 100 mg/L. In Figure 9, the separation efficiency decreases while the flow rate increases from 10 ml/min to 50 ml/min at constant magnetic flux density (B = 0,12 T). Raising the magnetic field density B from 0,06 T to 0,24 T at constant volume flow of 30 ml/min in Figure 10 involves the separation efficiency to increase.

Loading distribution of the matrix array

The loading distribution of a HGMS assembled with several matrix stages is important to be able to optimize the separation wire geometry. Figure 11 shows the deposited mass on each of the ten matrix steps along the filter length. The loading of the wire mesh at the inlet of the filter is the highest, declining in direction to the outlet. Clearly the difference between the

mesh geometries is visible; increasing dimensionless specific surface area Φ of the wire mesh induces that the load grows.

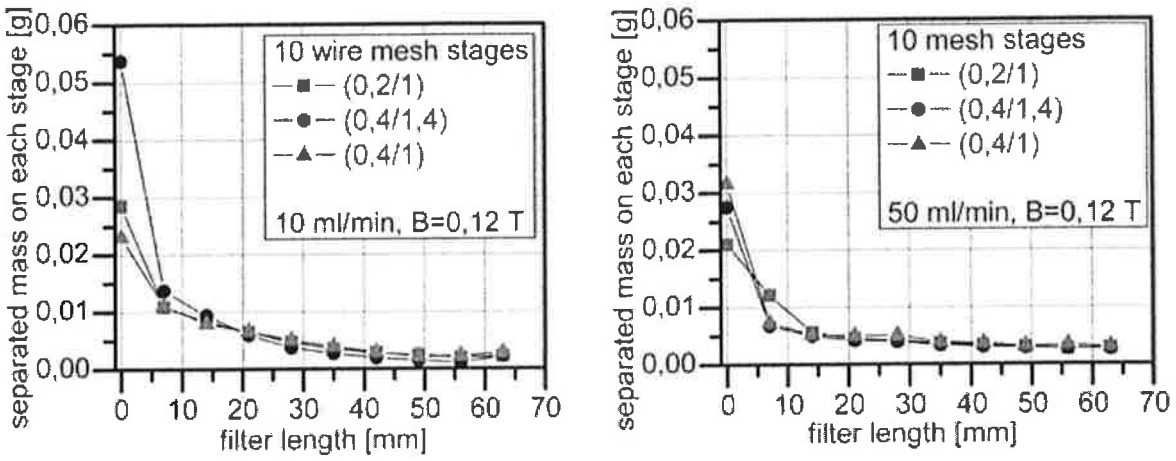

Figure 11: Loading gradient of mesh stages as a function of their position in the filter and the size of wire diameter *d* and mesh size *w*; left: 10 ml/min, right: 50 ml/min

Density distribution and separation grade

The previous results have shown the integral mass deposited on the wire mesh or the integral separation efficiency of the respective test. The grade efficiency gives the separation efficiency in dependency of the particle size. It is calculated as shown in the Method Section.

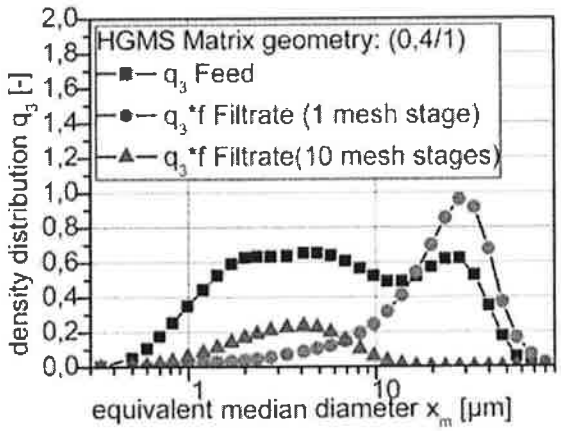

Figure 12: Density distribution of the particles in the feed, density distribution q_3 multiplied by the filtrate proportion *f* of the filtrate of two different experiments

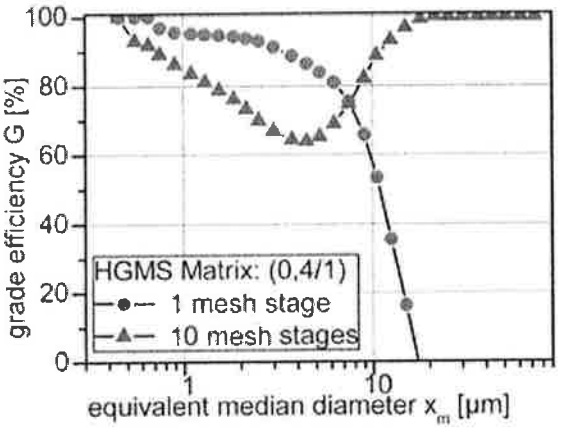

Figure 13: Grade efficiency of the test with one wire mesh stage and ten wire mesh stages

In Figure 12 the density distribution q_3 of the particles in the feed (rectangles symbols) and the density distribution q_3 multiplied by the filtrate proportion *f* from filtrate (q_3 * *f*) of two different experiments with one and ten mesh stages (circles and triangles symbols, respectively) are shown. The density distribution of particles in the feed shows that there are particles ranging from 0,5 µm to 80 µm.

The separation experiment with a single mesh stage (circles symbols) shows that the proportion of smaller sized particles declines sharply compared to the feed curve (q_3 feed, cubic symbol). Simultaneously the proportion of particles larger than 20 µm increased. This shows that the separation is inadequate if only one mesh stage is used. The magnetic gradient field inside the separation chamber causes the enlargement of the particles by a magnetically induced agglomeration.
Increasing the number of mesh stages to ten, which are mounted vertically in the filter at a distance of 5 mm between each other, involves that the largest particles are removed. The curve marked with triangle symbol shows that all particles larger than 18 µm are almost completely separated. In order to separate the remaining particles, the number of grid levels has to be increased further. The grade efficiency curves in Figure 13 complements the above mentioned observations.

5. Conclusion

The separation experiments using a single wire matrix stage show that the separation efficiency depends to a large extent on the geometry of the wire mesh. Increasing the dimensionless specific surface area Φ of the wire matrix, involves the enhancement of the separation efficiency. The experiments show that improving the separation efficiency of magnetic particles is achieved by reducing the velocity of the fluid and increasing the magnetic flux density of the background magnetic field. The number of wire matrix stages improves the separation efficiency. The first stage separates most of the particles. The measured size distributions of feed and filtrate show that the deposition and separation efficiency of one mesh stage is insufficient and causes the enlargement of the particles by magnetically induced agglomeration. Increasing the number of stages to ten units, which are mounted vertically in the filter, all particles larger than 18 µm are almost completely separated. In order to improve the separation of the remaining smaller particles, the number of mesh stages has to be increased further.

6. Acknowledgements

The authors owe special thanks to all organisations and companies supporting magnetic separation at the Institute of Mechanical Process Engineering and Mechanics (MVM). Among those are Haver and Boecker OHG, PALL GmbH, Drive Technology Research Union (FVA) and the Institute of Functional Interfaces (IFG) at KIT, Campus North. The research project IGF-No. 313 ZN was supported by funds from the Federal Ministry of Economics and Technology (BMWi) through the Industrial Research Associations "Otto von Guericke" e.V. (AiF).

REFERENCES

[1] DIN IEC 61400-4: *DIN IEC 61400-4 Wind turbines - Part 4: Design requirements for wind turbines gearboxes (IEC 88/354/CD:2009)/ Note: Date of issue 2010-05-10.* 2010

[2] GERBER, R. ; BIRSS, R.R. ; 58B STATION ROAD, Herts. SG6 3 BE E. Letchworth (Hrsg.): *High Gradient Magnetic Separation.* Research Studies Press, 1983

[3] KOPF, P. ; PIESCHE, M. ; SCHUETZ, S.: Beschreibung des Druckverlusts von Drahtgeweben mit Hilfe von Ähnlichkeitsgesetzen. In: *F&S Filtrieren und Separieren* 21 (2007), Nr. 6, S. 330–335